Experimental Charge Densities of Semiconducting Cage Structures Containing Alkaline Earth Guest Atoms**

Anders Bentien, Anders E. C. Palmqvist,
J. Daniel Bryan, Susan Latturner, Galen D. Stucky,
Lars Furenlid, and Bo B. Iversen*

Semiconducting clathrate structures (Figure 1) have recently stimulated much interest as potential thermoelectric energy converters.[1] A large number of elemental compositions can form clathrate type I structures, and frameworks of most Group 3, 4, and 5 elements have been made with guests from groups 1, 2, and 7.[2] Common to most of the compositions is the sum of the number of valence electrons of the elements present (184 e). Several studies have shown that the weakly bound guest atoms can exhibit extreme motion inside the oversized cavities.[3] This motion contributes to the reduction of the thermal conductivity of the clathrate materials, which is important for obtaining a high thermoelectric figure of merit (*ZT*).[4] Owing to the compositions of known clathrates there is a general belief that the guest atoms donate valence electrons to the framework atoms. Theoretical calculations surprisingly show that, contrary to common belief, the Sr guest atoms in $Sr_8Ga_{16}Ge_{30}$ appear neutral.[5] Clearly, it is important that this intriguing theoretical suggestion is validated by experiment. It is the subtle features of the host–guest interactions in framework materials, which to a large extent determine their highly desirable properties. Herein, we examine the structures, oxidation states, and host–guest interactions in two promising clathrates, $Sr_8Ga_{16}Ge_{30}$ and $Ba_8Ga_{16}Ge_{30}$, based on analysis of the X-ray electron density by using the maximum entropy method (MEM-ED analysis), and X-ray absorption near-edge structure (XANES) studies.

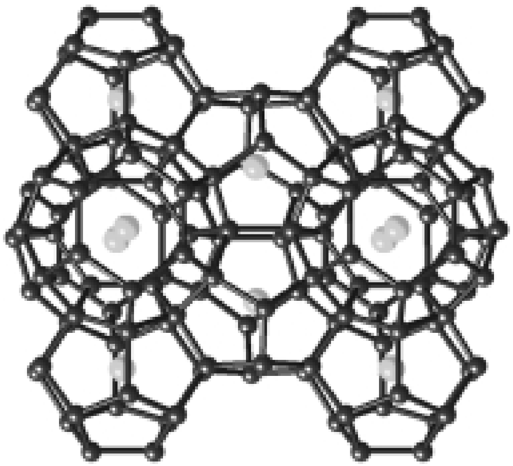

Figure 1. The clathrate type I structure. The two types of cages, the 20-atom dodecahedron and the 24-atom tetrakaidecahedron, are present in a 2:6 ratio in the unit cell. The guest atoms are located at (0,0,0) in the small cage, M(1), and at (1/4,1/2,0) in the large cage, M(2).

Figures 2 and 3 show the Sr K and the Ba L_{III} X-ray absorption edges for $Sr_8Ga_{16}Ge_{30}$ and $Ba_8Ga_{16}Ge_{30}$, respectively. The Sr in $Sr_8Ga_{16}Ge_{30}$ has a broad absorption edge with an energy similar to that of elemental Sr, and about 7 eV lower in energy than that of Sr^{II} in $Sr(OH)_2 \cdot 8\,H_2O$. The Ge K-edge energy in $Sr_8Ga_{16}Ge_{30}$ is equal to that of elemental Ge and 5 eV lower than in GeO_2, whereas the Ga K-edge is 1 eV higher than for elemental Ga and 4 eV lower than for Ga_2O_3. In contrast to Sr in $Sr_8Ga_{16}Ge_{30}$, the Ba in $Ba_8Ga_{16}Ge_{30}$ appears positively charged with an edge energy close to that of Ba^{II} in BaO. The Ge and Ga edges in $Ba_8Ga_{16}Ge_{30}$ have approximately the same values as in $Sr_8Ga_{16}Ge_{30}$. In summary the XANES data indicate that in $Ba_8Ga_{16}Ge_{30}$ the guest atoms donate electrons, whereas they appear more neutral in $Sr_8Ga_{16}Ge_{30}$. However, the different behavior of the guest atoms does not lead to appreciable differences in the framework absorption spectra within the resolution of the present experiments.

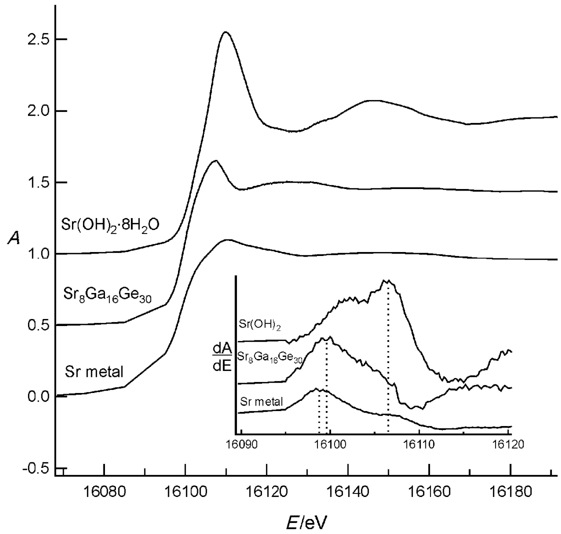

Figure 2. Sr K-edge XANES spectra of Sr metal, $Sr_8Ga_{16}Ge_{30}$, and $Sr(OH)_2 \cdot 8H_2O$. The abcissa shows the normalized absorption (*A*). The insert shows the derivative curves used to determine the edge energies (16099, 16100, and 16107 eV).

---

[*] Dr. B. B. Iversen, A. Bentien
Department of Chemistry
University of Aarhus
8000 Aarhus (Denmark)
Fax: (+45) 86196199
E-mail: bo@kemi.aau.dk

Dr. A. E. C. Palmqvist
Department of Applied Surface Chemistry
Chalmers University of Technology
412 96 Göteborg (Sweden)

J. D. Bryan, S. Latturner, Prof. G. D. Stucky
Department of Chemistry, University of California
Santa Barbara, CA 93106 (USA)

Dr. L. Furenlid
Department of Radiology and Optical Sciences Center
University of Arizona, Tucson, AZ 85724 (USA)

[**] Work at the X10c beamline at NSLS was supported by the Division of Materials Sciences of the US Department of Energy (DE-AC02-98CH10886). B.B.I. and A.E.C.P. gratefully acknowledge support from the Danish and Swedish Research Councils (SNF, TFR, STINT). This work was partially supported by the Office of Naval Research (G.D.S., J.D.B., S.L., A.E.C.P.), and it made use of MRL Central Facilities supported by the National Science Foundation under Award No. DMR96-32716. Dr. R. L. Paul of NIST is thanked for the Cold Neutron Prompt Gamma Ray Activation Analysis.

0044-8249/00/11220-3759 $ 17.50+.50/0

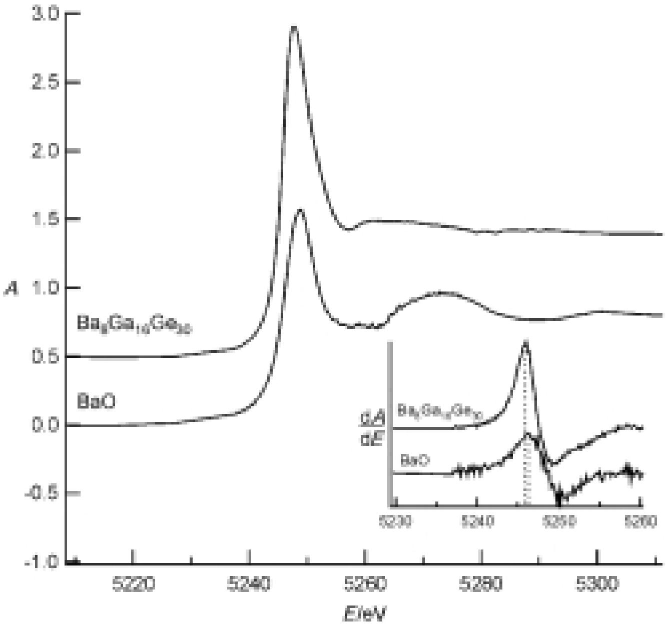

Figure 3. Ba L_{III}-edge XANES spectra of $Ba_8Ga_{16}Ge_{30}$ and BaO. The edge energy is 5246 eV for both samples.

The most conspicuous feature of the MEM-ED data of $Sr_8Ga_{16}Ge_{30}$ is the abnormally large smearing of the Sr(2) density. This feature must be due to large thermal motion or disorder of the Sr(2) guest atom, which is convoluted on the static density to give the smeared MEM density. In a single-crystal neutron diffraction study of $Sr_8Ga_{16}Ge_{30}$, Chakoumakos et al. found that the Sr(2) site is best modeled with four disordered sites.[6] Figure 4a shows the MEM deformation density (DD) of $Sr_8Ga_{16}Ge_{30}$. The insert shows the DD in the (100) plane, and it clearly reveals the Sr(2) disorder in the form of a torus-shaped density. It appears that the four-site disorder model is too simple an approximation for Sr(2). The MEM DD also suggests that the Sr(1) site is disordered. Figure 4b shows the MEM DD of $Ba_8Ga_{16}Ge_{30}$. Even though the Ba(2) guest atom is also diffuse compared with the other atoms in the structure, it has not been possible with least-squares modeling to refine a disordered Ba(2) site. However, the DD shows that the Ba(2) atom is disordered over four sites. As for $Sr_8Ga_{16}Ge_{30}$ there is furthermore evidence for disorder on the Ba(1) site. It is a virtue of the MEM that disorder does not need to be modeled explicitly. This makes it a strong tool in many materials research applications.

Theoretical calculations by Blake et al. suggest that the Sr atoms in $Sr_8Ga_{16}Ge_{30}$ are close to neutral and thus presumably have limited electronic interaction with the framework.[5] It is, however, very difficult to unambiguously define an atomic charge, and many definitions of atomic charge are in common use.[7] Attempts to refine monopolar charges on the atoms were unsuccessful. On the other hand the MEM-ED may allow an experimental estimation of the atomic charges by comparing the MEM densities with the nonuniform prior densities. These densities were constructed from assemblies of harmonically vibrating, neutral atoms, and the differences between the nonuniform priors and the MEM densities therefore provide an indication of the charge flow upon formation of the solids. Figure 5 shows a plot of the integrated charges as a function of spherical integration radii for $Sr_8Ga_{16}Ge_{30}$. Unfortunately the Sr(1) charge estimate is strongly affected by the few low-order reflections which suffer from extinction, as well as by the exact site occupancy. We have tested a number of models with various degrees of occupancy on the guest sites. As for the extinction, it is mostly the Sr(1) charge estimate which is affected by changes in the occupancy.[8] For comparison we have estimated atomic charges in NaF. It is notable that the method correctly retrieves positive Na and negative F, although the values are underestimated. In summary the MEM charge estimates support the XANES results with neutral Sr(2) atoms in $Sr_8Ga_{16}Ge_{30}$. However, owing to the combined effects of extinction and partial occupancy we have not been able to obtain reliable MEM charge estimates for Sr(1) and the Ba atoms in $Ba_8Ga_{16}Ge_{30}$.

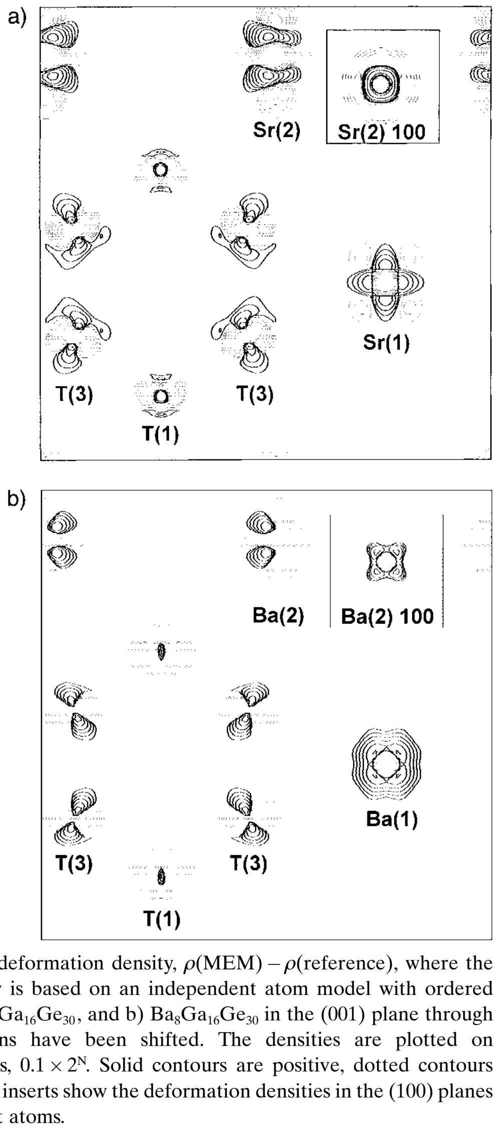

Figure 4. MEM deformation density, $\rho(\text{MEM}) - \rho(\text{reference})$, where the reference density is based on an independent atom model with ordered guest sites. a) $Sr_8Ga_{16}Ge_{30}$, and b) $Ba_8Ga_{16}Ge_{30}$ in the (001) plane through $z = 0$. The origins have been shifted. The densities are plotted on logarithmic scales, 0.1×2^N. Solid contours are positive, dotted contours are negative. The inserts show the deformation densities in the (100) planes of the M(2) guest atoms.

The exact framework siting of the Ga and Ge atoms is known to be very important for the thermoelectric properties of clathrate materials.[5] Refinement of framework occupancies results in random distributions for both compounds. This

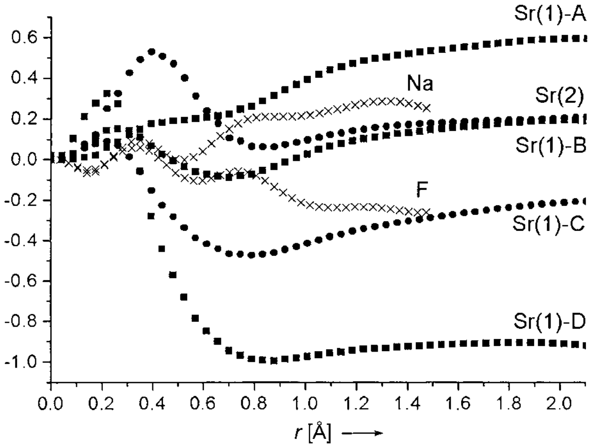

Figure 5. Spherical integration around the guest atom positions of the difference between the nonuniform prior density and the MEM density in $Sr_8Ga_{16}Ge_{30}$. For Sr(1) four charge estimates are shown. A) The five most extinction corrected data removed (006, 222, 035, 123, 004) and 100% Sr(1) occupancy; B) as A) but refined Sr(1) occupancy (98.6%); C) all data and refined Sr(1) occupancy; D) as A) but 95% Sr(1) occupancy. For Sr(2) the charge estimate is nearly constant between models, and the plot is based on B). Results obtained from MEM analysis of literature data on NaF are also included.[16] q = atomic charge; r = radius.

could be real, but it could also be because the difference between the Ga and Ge EDs in the clathrate is too small to distinguish. Differentiation between Ga and Ge may be further hindered if the Ga atoms receive electrons from the guest atoms. Figure 6 shows the integrated difference density for the three framework sites. The plot shows that relative to the reference models having random distributions of neutral Ga and Ge atoms, the 6c sites are depleted of electrons and the 16i sites have a charge accumulation. This indicates that Ga preferentially occupies the non-tetrahedral 6c sites (6-rings), and avoids the tetrahedral 16i sites. This siting also leads to fewer Ga–Ga contacts, which have been shown by theory to be energetically unfavorable.[5] The plot suggests that the difference from a random siting model is smaller for $Ba_8Ga_{16}Ge_{30}$ than for $Sr_8Ga_{16}Ge_{30}$. This indirectly supports the XANES data, which show that Ba is more positively charged in the clathrates than Sr.

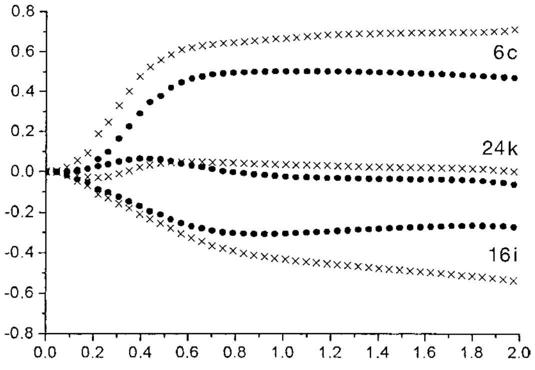

Figure 6. Spherical integration around the framework positions of the difference between nonuniform prior densities corresponding to random Ga/Ge distributions and the MEM densities. The crosses are $Sr_8Ga_{16}Ge_{30}$ and the circles $Ba_8Ga_{16}Ge_{30}$. For $Sr_8Ga_{16}Ge_{30}$ the framework atoms are located at 6c(0.25, 0, 0.5), 16i(0.18913, 0.18913, 0.18913), and 24k(0, 0.30914, 0.11731). q = atomic charge; r = radius.

It is clear that the host–guest interactions in these clathrate materials are highly tunable and are a key ingredient for the understanding of thermoelectric and transport properties. The present study demonstrates the ability of framework structures to selectively modify the chemical behavior of guest species. Such abilities are widely used in, for example, zeolite catalysts, but it appears that the chemistry of guest species trapped in framework systems is richer than conventionally believed based on simple chemical arguments. The fact that the guest atoms are not fully ionized and may have partial occupancy also suggests that the framework can have a range of Ga/Ge compositions.

Experimental Section

Synthesis: In a high-purity Ar-filled dry box, stochiometric amounts of alkaline earth element (Cerac, > 99.7% purity) and Ge (Cerac, > 99.999% purity) were placed in a quartz tube along with a large excess of Ga (Cerac, 99.99% purity). The reaction mixtures were heated at 3.0 $K\,min^{-1}$ to 1100 °C and held at this temperature for one hour. The reactions were then cooled at 0.3 $K\,min^{-1}$ to their respective melting points. Each reaction was then annealed for 100 h at 10 °C below their melting point. After the annealing procedure each reaction was cooled at 1 $K\,min^{-1}$ to room temperature. The air-stable crystal/gallium matrix was removed from the quartz tubes and placed in an evaporating dish on a hot plate to keep the gallium molten. The crystals were then plucked out of the liquid gallium with tweezers and placed into a bath of concentrated hydrochloric acid for several days to dissolve the remaining gallium.

The composition of single crystals of $Sr_8Ga_{16}Ge_{30}$ and $Ba_8Ga_{16}Ge_{30}$ was determined by electron microprobe analysis using a Cameca SX-50 with standard settings. Calibration was made by using geologic mineral standards of known composition and elemental gallium (Cerac 99.999%). The compositions by weight: $Sr_8Ga_{16}Ge_{30}$: 17.13% Sr, 27.33% Ga, 56.01% Ge; $Ba_8Ga_{16}Ge_{30}$: 25.25% Ba, 24.55% Ga, 49.64 Ge. This correlates to $Sr_{7.73}Ga_{15.50}Ge_{30.50}$ and $Ba_{8.16}Ga_{15.63}Ge_{30.36}$, respectively. An error of no greater than 3.4% from the ideal 8:16:30 stoichiometry is observed for the Sr clathrate and 2.3% for the Ba clathrate. The observed error is a result of slight deviations in the take-off-angle of the emitted X-rays from the near orthogonal crystal faces sampled. This stoichiometry gives 183.96 and 184.65 valence electrons for the Sr and Ba clathrates, respectively, and thus the structures are believed to be free of defects.

Cold neutron gamma ray activation analysis provided by the National Institute of Standards and Technology (NIST) was used to monitor hydrogen absorption of the $Sr_8Ga_{16}Ge_{30}$ clathrate during the isolation procedure. Samples isolated by acid dissolution of the Ga flux were compared to a control sample isolated by sonication in the absence of acid. Emission of gamma rays, monitored by a high-purity germanium detector, allows the de-excitation of the complex nuclei formed from the neutron capture event. The control sample measured 0.018(5) $counts\,s^{-1}$, while the sample isolated from acid measured 0.013(3) $counts\,s^{-1}$. These results indicate that no hydrogen is present within any of the samples.

X-ray absorption spectroscopy: XANES measurements were carried out at beamline X10C at the NSLS, Brookhaven National Laboratory. The K-edges of Ga, Ge, and Sr, and the L_{III} edge of Ba, were studied in transmission mode on powdered samples evenly smeared on to scotch tapes, which were folded into eight layers to ensure even sample distributions without pinholes. Elemental as well as oxidized standards (Sr, $Sr(OH)_2 \cdot 8H_2O$, BaO, Ga, Ga_2O_3, Ge, and GeO_2) were used as references for the photon energy scales at the absorption edges, which were scanned by using 0.2 eV steps. The elemental Sr was sealed under argon in aluminized Mylar film. The data were analyzed by using the MacXAFS3.6 software package,[9] and absorption edge energies were determined at the maximum values of the derivatives of the absorption curves.

X-ray diffraction: Tube measurements were done at room temperature on a Bruker SMART CCD diffractometer ($Mo_{K\alpha}$). Data collection and integration was carried out with the SMART software. Averaging and empirical absorption corrections were carried out with SADABS.[10] Least-squares refinements were made with programs LINEX[11] and XD[12] in the space group $Pm\bar{3}n$. For both structures free refinement of framework atom occupancies resulted in random distributions of Ga and Ge atoms. Refinement of guest atoms occupancies showed all sites to be fully occupied except Sr(1), which refined to 98.6(4)% occupancy. In both refinements anisotropic thermal parameters were employed on all atoms as well as isotropic extinction parameters. For $Sr_8Ga_{16}Ge_{30}$ a split-atom model was used for Sr(2) as in reference [6] ($(x, y, z) = (0, 0.4784, 0.9784)$). $Sr_8Ga_{16}Ge_{30}$ [$Ba_8Ga_{16}Ge_{30}$]: $a = 10.740(2)$ [10.785(2)] Å, $V = 1238.7(1)$ [1254.4(1)] Å^3, $V_{crystal} = 0.0004$ [0.0003] mm^3, $\rho_{calcd} = 5.354$ [5.791] g cm^{-3}, $\lambda = 0.7107$ Å, $(\sin\theta/\lambda)_{max} = 0.923$ [0.836] Å^{-1}, $\mu_l = 345$ [322] cm^{-1}, T_{max}, $T_{min} = 0.2060, 0.0883$ [0.2534, 0.1132], no. of measured reflections = 35927 [54576], no. of unique = 691 [558], $R_w(\text{int}) = 0.0451$ [0.0361], $N_{obs} = 691$ [558] ($I > 0\sigma(I)$), $N_{par} = 19$ [16], GOF = 0.40 [0.52], $R_{F^2} = 0.0256$ [0.0170], $R_{wF^2} = 0.0254$ [0.0169], Y_{min}(extinction) = 0.79 [0.81] (10 and 8 reflections have $Y < 0.95$). Further details on the crystal structure investigations may be obtained from the Fachinformationszentrum Karlsruhe, 76344 Eggenstein-Leopoldshafen, Germany (fax: (+49) 7247-808-666, on quoting the depository numbers CSD-411062 ($Sr_8Ga_{16}Ge_{30}$) and CSD-411063 ($Ba_8Ga_{16}Ge_{30}$)).

MEM calculations: Absorption, extinction, and anomalous dispersion-corrected observed structure factors phased and scaled with program XD were used for MEM calculations with the MEED program.[13] The calculations employed nonuniform prior densities obtained by a structure factor aliasing procedure[14] proposed by Roversi et al.[15] This method is superior to straightforward Fourier transformation, which gives series termination ripples. In the present calculations 28 structure factor copies were used with a cut-off value of 10^{-9}. The nonuniform priors correspond to the EDs of assemblies of neutral atoms having anisotropic harmonic thermal motion. This means that the observed data are used to estimate the effects of chemical bonding, charge transfer, and disorder. For $Sr_8Ga_{16}Ge_{30}$ the MEM density was almost unchanged between calculations with nonuniform priors having ordered and disordered (i.e. split) Sr(2) sites. In all MEM calculations a $128 \times 128 \times 128$ pixel grid was used and iterations were stopped at $\chi^2 = 1$. Estimated standard uncertainties on the structure factors were obtained from the data averaging procedure.

Received: December 21, 1999
Revised: August 3, 2000 [Z 14432]

---

[1] F. J. DiSalvo, *Science* **1999**, *285*, 703–706.
[2] a) J. S. Kasper, P. Hagenmuller, M. Pouchard, *Science* **1965**, *150*, 1713–1714; b) v. H. Menke, H. G. von Schnering, *Z. Anorg. Allg. Chem.* **1973**, *395*, 223–238; c) B. Eisenmann, H. Schäfer, R. Zagler, *J. Less-Comm. Met.* **1986**, *118*, 43–55.
[3] B. C. Sales, B. C. Chakoumakos, D. Madrus, J. W. Sharp, *J. Solid State. Chem.* **1999**, *146*, 528–532.
[4] The thermoelectric figure of merit is defined as $ZT = TS^2\sigma/\kappa$, where S is the Seebeck coeffient, σ the electrical conductivity, and κ the thermal conductivity.
[5] N. P. Blake, L. Møllnitz, G. Kresse, H. Metiu, *J. Chem. Phys.* **1999**, *111*, 3133–3144.
[6] B. C. Chakoumakos, B. C. Sales, D. G. Mandrus, G. S. Nolas, *J. Alloys Compd.* **2000**, *296*, 80–86.
[7] P. Coppens, *X-ray charge densities and chemical bonding*, Oxford University Press, Oxford, **1997**.
[8] The occupancy of the guest sites can only be *less* than 100%, and thus partial occupancy on Sr(2) can only make the charge estimate more negative. Changing the occupancy on Sr(2) has little effect on the charge estimate, but for Sr(1) it alters the estimate significantly. However, changes in the Sr(1) occupancy also degrades the crystallographic R factors (e.g. $R(F^2) = 0.0274$ (95%), $R(F^2) = 0.0256$ (98.6%)).
[9] MacXAFS3.6 Software Package, C. E. Bouldin, W. T. Elam, L. Furenlid, *Physica B* **1995**, *208*, 190–192.
[10] Owing to the enormous redundancy of the data, empirical absorption corrections were found to give much better results than corrections based on approximate analytical crystal shapes.
[11] P. Coppens, Program LINEX, Department of Chemistry, State University of New York at Buffalo, New York 14260, **1974**.
[12] T. Koritsanszky, S. T. Howard, P. R. Mallison, Z. Su, T. Richter, N. K. Hansen, Program XD, Institute of Crystallography, Freie Universität, Berlin, Germany, **1999**. The program was locally modified to handle atoms with $Z > 36$ by Dr. Piero Macchi.
[13] S. Kumazawa, Y. Kubota, M. Takata, M. Sakata, Y. Ishibashi, *J. Appl. Crystallogr.* **1993**, *26*, 453–457.
[14] A. Bentien, Program ASF, Department of Chemistry, University of Aarhus, 8000 Aarhus C, Denmark, **2000**.
[15] P. Roversi, J. J. Irwin, G. Bricogne, *Acta Crystallogr. Sect. A* **1998**, *54*, 971–996.
[16] C. J. Howard, R. D. G. Jones, *Acta Crystallogr. Sect. A* **1977**, *33*, 776.

Self-Assembly of Pentameric Porphyrin Light-Harvesting Antennae Complexes**

Richard A. Haycock, Arkady Yartsev,
Ulrike Michelsen, Villy Sundström, and
Christopher A. Hunter*

The reaction centers of natural photosynthetic systems are excited indirectly through their light-harvesting antennae complexes.[1–3] These units contain a network of chromophores which absorb light energy and channel this very efficiently by singlet energy transfer to the photochemical reaction centres.[4, 5] The photochemical properties of porphyrins lend themselves to the design of artificial organic antennae systems,[6] and covalently linked arrays of five or more porphyrins have been constructed.[7–10] We demonstrate here that cooperative self-assembly processes are ideally suited to the construction of stable structurally well-defined chromophore arrays for use as antennae systems.[11, 12]

Zn$_2$1 and **H$_2$2** were designed to be perfectly complementary, preorganized partners for the self-assembly process shown in Scheme 1.[13] Intramolecular hydrogen bonds constrain both molecules to essentially one conformation, thus minimizing the loss of rotational entropy upon binding. The spacing of the coordination sites ensures that **Zn$_2$1** will coordinate to the *trans-meso* ligands across the face of **H$_2$2** with no strain in the final complex.[14] The central free-base porphyrin is encapsulated in a spherical array of four zinc

---

[*] Prof. C. A. Hunter, Dr. R. A. Haycock, Dr. U. Michelsen
Krebs Institute for Biomolecular Science
Department of Chemistry
University of Sheffield
Sheffield S3 7HF (UK)
Fax: (+44) 114-273-8673
E-mail: C.Hunter@shef.ac.uk

Dr. A. Yartsev, Prof. V. Sundström
Department of Chemistry
University of Lund
Lund (Sweden)

[**] We thank the EPSRC (R.A.H.) and the Lister Institute (C.A.H.) for funding. V.S. and A.Y. thank the Swedish NFR and the K&A Wallenberg Foundation for financial support.